

1 **Uncovering the hidden antibiotic potential of Cannabis**

2
3

4 Maya A. Farha^{1,2, †}, Omar M. El-Halfawy^{1,2,3, †}; Robert T. Gale^{1,2}; Craig R. MacNair^{1,2}; Lindsey A.
5 Carfrae^{1,2}; Xiong Zhang^{1,2}, Nicholas G. Jentsch^{1,2}; Jakob Magolan^{1,2}; Eric D. Brown^{1,2*}

6

7 ¹ Department of Biochemistry and Biomedical Sciences, McMaster University, Hamilton, Ontario L8N
8 3Z5, Canada

9 ² Michael G. DeGroot Institute of Infectious Disease Research, McMaster University, Hamilton,
10 Ontario, L8N 3Z5, Canada

11 ³ Microbiology and Immunology Department, Faculty of Pharmacy, Alexandria University,
12 Alexandria, 21521, Egypt

13 * To whom correspondence should be addressed (ebrown@mcmaster.ca)

14 † These authors contributed equally

15
16

17

18

19

20

21

22

23

24

25 **Abstract**

26

27 The spread of antimicrobial resistance continues to be a priority health concern worldwide,
28 necessitating exploration of alternative therapies. *Cannabis sativa* has long been known to contain
29 antibacterial cannabinoids, but their potential to address antibiotic resistance has only been
30 superficially investigated. Here, we show that cannabinoids exhibit antibacterial activity against
31 MRSA, inhibit its ability to form biofilms and eradicate stationary phase cells persistent to antibiotics.
32 We show that the mechanism of action of cannabigerol is through targeting the cytoplasmic membrane
33 of Gram-positive bacteria and demonstrate *in vivo* efficacy of cannabigerol in a murine systemic
34 infection model caused by MRSA. We also show that cannabinoids are effective against Gram-negative
35 organisms whose outer membrane is permeabilized, where cannabigerol acts on the inner membrane.
36 Finally, we demonstrate that cannabinoids work in combination with polymyxin B against multi-drug
37 resistant Gram-negative pathogens, revealing the broad-spectrum therapeutic potential for
38 cannabinoids.

39

40

41

42

43

44

45

46

47

48

49

50

51

52

53

54

55

56

57

58

59

60

61

62 Public Health agencies around the globe have identified antimicrobial resistance as one of the
63 most critical challenges of our time. The rapid and global spread of antimicrobial-resistant organisms in
64 recent years has been unprecedented. So much so that the world health organization (WHO) published
65 its first ever list of antibiotic-resistant "priority pathogens", made up of 12 families of bacteria that pose
66 the greatest threat to human health¹. Among them, *Staphylococcus aureus* is the leading cause of both
67 healthcare and community-associated infections worldwide and a major cause for morbidity and
68 mortality², especially with the emergence and rapid spread of methicillin-resistant *S. aureus* (MRSA),
69 which is resistant to all known β -lactam antibiotics³. Worse yet, resistance to vancomycin, linezolid
70 and daptomycin has already been reported in MRSA clinical strains, compromising the therapeutic
71 alternatives for life-threatening MRSA infections⁴. Further, antibiotic-resistant Gram-negative
72 infections have increasingly become a pressing issue in the clinic. Indeed, of the bacteria highlighted
73 by the WHO, 75% are Gram-negative organisms. Among the currently approved antibiotics, the latest
74 discovery of a new drug class dates back to more than 30 years ago. The rapid loss of antibiotic
75 effectiveness and diminishing pipeline beg for the exploration of alternative therapies.

76 *Cannabis* plants are important herbaceous species that have been used in folk medicine since
77 the dawn of times. Increasing scientific evidence is accumulating for the efficacy of its metabolites in
78 the treatment, for example, of epilepsy, Parkinson disease, analgesia, multiple sclerosis, Tourette's
79 syndrome and other neurological diseases⁵. At a very nascent stage are investigations into the potential
80 of cannabis metabolites as antibacterial therapies. To date, assessments of their antibacterial activity
81 have been few and superficial. *In vitro* studies have shown cannabinoids inhibit the growth of Gram-
82 positive bacteria, mostly *S. aureus*, with no detectable activity against Gram-negative organisms⁶⁻⁹,
83 where the clinical need is highest. Further, the mechanism of action has remained elusive and there has
84 been little validation of antibacterial activity *in vivo*.

85 Here, we show that cannabinoids exhibit antibacterial activity against MRSA, inhibit its ability
86 to form biofilms and eradicate stationary phase cells persistent to antibiotics. We show that the
87 mechanism of action of cannabigerol (CBG) is through targeting the cytoplasmic membrane of Gram-
88 positive bacteria and demonstrate *in vivo* efficacy of CBG in a murine systemic infection model caused
89 by MRSA. We also show that cannabinoids are effective against Gram-negative organisms whose outer
90 membrane is permeabilized, where CBG acts on the inner membrane. Finally, we demonstrate that
91 cannabinoids work in combination with polymyxin B against multi-drug resistant Gram-negative
92 pathogens, revealing the broad-spectrum therapeutic potential for cannabinoids. In all, our findings

93 position cannabinoids as promising leads for antibacterial development that warrant further study and
94 optimization.

95

96 **Results and Discussion**

97

98 We began our study investigating the antibacterial, anti-biofilm and anti-persister activity of a
99 variety of commercially available cannabinoids, including the five major cannabinoids,
100 cannabichromene (CBC), cannabidiol (CBD), cannabigerol (CBG), cannabinol (CBN), and Δ^9 -
101 tetrahydrocannabinol (THC), as well as a selection of their carboxylic precursors (pre-cannabinoids)
102 and other synthetic isomers (18 unique molecules total) against methicillin-resistant *S. aureus* (MRSA)
103 (Supplementary Table 1). Susceptibility tests were conducted according to the Clinical and Laboratory
104 Standards Institute (CLSI) protocol against MRSA USA300, a highly virulent and prevalent
105 community-associated MRSA. Overall, antibacterial activities for the five major cannabinoids (and
106 some of their synthetic derivatives) were in line with previously published work⁶⁻⁸. Seven molecules
107 were potent antibiotics with minimum inhibitory concentration (MIC) values of 2 $\mu\text{g/mL}$, including
108 CBG, CBD, CBN, cannabichromenic acid (CBCA) and THC along with its Δ^8 - and exo-olefin
109 regioisomers. We observed moderate loss of potency associated with the benzoic acid moiety (CBG,
110 CBD, and THC were more potent than CBGA, CBDA, THCA) and when n-pentyl substituent was
111 replaced with n-propyl (CBD and THC were superior to CBDV and THCV) (Supplementary Table 1).
112 These two modifications appeared to have an additive detrimental effect on antibacterial activity
113 (THCVA, CBDVA). Two other THC derivatives, (\pm) 11-nor-9-carboxy- Δ^9 -THC, and (\pm) 11-hydroxy-
114 Δ^9 -THC, as well as cannabicylol were inactive at the highest concentrations screened (MIC > 32
115 $\mu\text{g/mL}$) (Supplementary Table 1).

116 Biofilm formation by MRSA, typically on necrotic tissues and medical devices, is considered
117 an important virulence factor influencing its persistence in both the environment and the host
118 organism¹⁰. These highly structured surface-associated communities of MRSA are typically associated
119 with increased resistance to antimicrobial compounds and are generally less susceptible to host immune
120 factors. We assessed the ability of the various cannabinoids to inhibit the formation of biofilms by
121 MRSA, using static abiotic solid-surface assays in which MRSA was treated with increasing
122 concentrations of cannabinoids under conditions favouring biofilm formation (Supplementary Fig. 1).
123 In all, the degree of inhibition of biofilm formation correlated with antibacterial activity; those
124 cannabinoids with potent activity against MRSA strongly suppressed biofilm formation and vice versa
125 (Supplementary Fig. 1, Supplementary Table 1). The five major cannabinoids clearly repressed MRSA
126 biofilm formation, with CBG (Fig. 1a) exhibiting the most potent anti-biofilm activity. Indeed, as little

127 as 0.5 µg/mL (1/4 MIC) of CBG inhibited biofilm formation by ~50% (Fig. 1b). Thus, this experiment
128 underlined the strong inhibitory effect of cannabinoids on biofilm formation; this sub-MIC level of
129 CBG did not affect planktonic growth.

130 Another challenge in the treatment of MRSA infections is the formation of non-growing,
131 dormant ‘persister’ subpopulations that exhibit high levels of tolerance to antibiotics¹¹⁻¹³. Persister cells
132 have a role in chronic and relapsing *S. aureus* infections¹⁴ such as osteomyelitis¹⁵, and endocarditis¹⁶.
133 Here, we evaluated the killing activity of a series of cannabinoids against persisters derived from
134 stationary phase cells of MRSA USA300 (Supplementary Fig. 2). These have been previously shown to
135 be tolerant to conventional antibiotics such as gentamicin, ciprofloxacin and vancomycin^{11, 17-18}. In
136 general, the anti-persister activity correlated with potency against actively dividing cells as determined
137 by MIC assays (Supplementary Table 1). Again, CBG was the most potent cannabinoid against
138 persisters, whereas oxacillin and vancomycin were ineffective at concentrations that otherwise kill
139 actively dividing cells (Supplementary Fig. 2, Fig. 1c). More specifically, CBG killed persisters in a
140 concentration-dependent manner starting at 5 µg/ml. Notably, CBG rapidly eradicated a population of
141 ~10⁸ CFU/ml MRSA persisters to below the detection threshold within 30 minutes of treatment (Fig.
142 1c).

143 We selected CBG (Fig.1a) for further studies of mechanism and *in vivo* efficacy. Not only did
144 CBG potently inhibit MRSA, repress biofilm formation (Fig. 1b) and effectively eradicate persister
145 cells (Fig. 1c), but it is non-psychotropic, non-sedative and constitutes a component of *Cannabis* for
146 which there is high therapeutic interest¹⁹. Further, we were also able to synthesize CBG efficiently
147 from olivetol and geraniol, two inexpensive precursors, in one synthetic operation. We were cognisant
148 that such facile synthetic access would enhance the potential for subsequent medicinal chemistry-based
149 development efforts. We determined the MIC₉₀ of CBG against 96 clinical isolates of MRSA using the
150 CLSI protocol. The corresponding frequency distribution of MICs is presented in Fig. 1d. Overall, the
151 MICs ranged from 0.0625 – 8 µg/mL with a resulting MIC₉₀ of 4 µg/mL. This activity compares
152 favourably with conventional antibiotics for these multi-drug resistant strains.

153 Given its growth inhibitory action on Gram-positive bacteria, we reasoned isolating resistant
154 mutants to CBG would be a straightforward approach to gather insights into its bacterial target. Indeed,
155 resistance mutations can often be mapped to a drug's molecular target²⁰. To this end, MRSA was
156 repeatedly challenged with various lethal concentrations of CBG, ranging from 2-16x MIC, to select
157 for spontaneous resistance in MRSA (Fig. 2). No spontaneously resistant mutants were obtained,
158 indicating a frequency of resistance less than 10⁻¹⁰ for MRSA. We also attempted to allow MRSA
159 bacteria to develop resistance to CBG by sequential subcultures via 15-day serial passage in liquid

160 culture containing sub-MIC concentrations of CBG and, again, no change in the MIC of CBG was
161 detected (Fig. 2). While these experiments were unsuccessful probes of mechanism, they suggested
162 very low rates of resistance for CBG, a highly desirable property for an antibiotic.

163 We turned to chemical genomic analysis to generate hypotheses for the target of CBG. Such
164 studies can reveal patterns of sensitivity among genetic loci that are characteristic of the mechanism of
165 action of an antibacterial compound²¹. We confirmed that the model Gram-positive bacterium *B.*
166 *subtilis* was susceptible to CBG (MIC 2 µg/mL), and screened a CRISPR interference knockdown
167 library, of all essential genes in *B. subtilis*²² for further sensitization to CBG. In the absence of
168 induction, relying on basal repression (which leads to a ~3-fold repression of the knockdown library²²),
169 we were unable to detect any knockdowns sensitized to sub-lethal concentrations of CBG (Fig. 2).
170 Low-level induction identified some sensitive and some suppressing clones, however follow-on work
171 with the individual knockdowns in liquid culture via full checkerboard analysis (combining xylose, the
172 inducer, with CBG) failed to confirm sensitivity or suppression. In all, we were unable to identify *bona*
173 *fide* chemical genetic interactions among essential genes of *B. subtilis* and CBG. We next aimed to
174 query the non-essential gene subset, this time using the Nebraska Transposon Mutant Library, a
175 sequence-defined transposon mutant library consisting of 1,920 strains, each containing a single
176 mutation within a nonessential gene of CA-MRSA USA300²³, again looking for genetic enhancers or
177 suppressors to generate target hypotheses (Fig. 2, Supplementary Fig. 3a). While we were unable to
178 uncover genetic suppressors at supra-lethal concentrations of CBG, we identified 41 transposons as
179 sensitive across 3 different sub-lethal concentrations of CBG (Supplementary Table 2). Analysis of
180 these transposons revealed a significant enrichment for genes encoding proteins that are localized at the
181 cytoplasmic membrane (Supplementary Fig. 3b) and enrichment for genes encoding functions in
182 processes that take place at the cytoplasmic membrane, such as cellular respiration and electron
183 transport chain (Supplementary Fig. 3c). In all, chemical genomic profiling with CBG generally linked
184 its activity to cytoplasmic membrane function.

185 The lack of clear targets among the essential gene products, the predominance of chemical
186 genetic interactions linked to membrane function, and the difficulty generating resistant mutants,
187 suggested that CBG might act on the cytoplasmic membrane of MRSA. Indeed, the propensity of
188 membrane-active compounds to generate resistance is frequently low²⁴. Further, the bacterial
189 membrane is critical for cell function and survival, and is essential irrespective of the metabolic status
190 of the cell, including non-growing and persisting cells²⁴. The strong action of CBG on persister cells
191 would be consistent with such a mode of action. Thus, we assessed the ability of CBG to disrupt
192 membrane function using the membrane potential-sensitive probe, 3,3'-dipropylthiadicarbocyanine

193 iodide (DiSC₃(5)). In DiSC₃-loaded MRSA cells, CBG caused a dose-dependent increase in
194 fluorescence that occurred at a concentration consistent with the MIC of CBG (Fig. 2). To probe the
195 possibility that CBG selectively dissipated membrane potential ($\Delta\psi$) component of proton motive
196 force, we tested for synergy with sodium bicarbonate, a known perturbant of ΔpH , that has been shown
197 to synergize with molecules that reduce $\Delta\psi$ ²⁵. A lack of synergy between these compounds suggested
198 CBG disrupts the integrity of the cytoplasmic membrane (Supplementary Fig. 4).

199 Having established strong *in vitro* potency for CBG against MRSA, we next sought to evaluate
200 the *in vivo* efficacy in a murine systemic infection model of MRSA. The effect of CBG on a systemic
201 infection mediated by the CA-MRSA USA300 strain is shown in Fig. 3. Given that no signs of acute
202 toxicity were reported in a pharmacokinetic study of 120-mg/kg doses of CBG²⁶, we used a dose of 100
203 mg/kg in this study. CBG displayed a significant reduction in bacterial burden in the spleen by a factor
204 of 2.8- \log_{10} in CFU compared to the bacterial titer seen with the vehicle ($p < 0.001$, Mann-Whitney *U*-
205 test). Overall, CBG displayed promising levels of efficacy in the systemic infection model.

206 To date, antibacterial activity of cannabinoids against Gram-negative organisms has largely
207 been ruled out, since reported MICs values fall in the 100-200 $\mu\text{g/mL}$ range⁷⁻⁸. We confirmed this,
208 obtaining MICs $>128 \mu\text{g/mL}$ for all of the tested cannabinoids against the model Gram-negative
209 organism *Escherichia coli*. Given the observed action of CBG on the cytoplasmic membrane of MRSA,
210 we reasoned that CBG (and other cannabinoids) might be equally effective on the Gram-negative
211 counterpart, the inner membrane. Further, just as many antibacterial compounds fail to work against
212 Gram-negative pathogens due to a permeability barrier²⁷, we reasoned that low permeability across the
213 outer membrane (OM) may be the reason for the poor efficacy of cannabinoids. Thus, we investigated
214 the antibacterial profile of the five major cannabinoids against *E. coli*, where their permeation was
215 facilitated through the OM by means of chemical perturbation. To this end, we set up checkerboard
216 assays to assess the interaction of CBG (Fig. 4a) and the four other main cannabinoids (Supplementary
217 Fig. 5) with the membrane perturbant, polymyxin B against *E. coli*. Remarkably, all five major
218 cannabinoids gained potent activity in the presence of sub-lethal concentrations of polymyxin B.
219 Indeed, all interactions were deemed synergistic (Fig. 4, Supplementary Fig. 5). For example, CBG,
220 which was inactive against *E. coli* ($>128 \mu\text{g/mL}$), was strongly potentiated when combined with a sub-
221 lethal concentration of polymyxin B (1 $\mu\text{g/mL}$ in the presence of 0.062 $\mu\text{g/mL}$ polymyxin B). We
222 further assessed whether OM perturbation by genetic means would lead to similar results by evaluating
223 the activity of CBG against a number of strains where the OM was compromised (Fig. 4b). In an *E. coli*
224 $\Delta\text{bamB}\Delta\text{tolC}$ deletion strain, which renders *E. coli* hyperpermeable to many small molecules, due to
225 loss of BamB, a component of the β -barrel assembly machinery for OM proteins and TolC, the efflux

226 channel in the outer membrane, CBG had a MIC of 4 $\mu\text{g}/\text{mL}$, on par with its Gram-positive activity.
227 Similarly, in a hyperporinated, $\Delta 9$ strain of *E. coli*, where a recombinant pore was introduced in the
228 OM and all nine known TolC-dependent transporters deleted²⁸, CBG activity became evident with a
229 MIC of 8 $\mu\text{g}/\text{mL}$. Finally, in an *Acinetobacter baumannii* deficient in lipooligosaccharide (LOS-),
230 which effectively alters the permeability of the OM²⁹, CBG activity was enhanced greater than 128-
231 fold, resulting in a MIC value of 0.5 $\mu\text{g}/\text{mL}$. Overall, these results suggest that cannabinoids face a
232 permeability barrier in Gram-negative bacteria and further imply that cannabinoids inhibit a bacterial
233 process present in Gram-negative pathogens, and likely common to that in Gram-positive pathogens.

234 To this end, we investigated whether CBG acted on the inner membrane (IM) of *E. coli* as well
235 as the OM, presumably as a consequence of nonspecific membrane effects, as reported for many
236 membrane-active agents. IM and OM permeability were determined, respectively, from ortho-
237 Nitrophenyl- β -galactoside (ONPG) and nitrocefin hydrolysis in an *E. coli* strain constitutively
238 expressing a cytoplasmic β -galactosidase and a periplasmic β -lactamase while lacking the lactose
239 permease, as described in the literature³⁰. As shown in Fig. 4c, CBG specifically acted on the IM, and
240 only in the presence of polymyxin B at a sub-lethal concentration that had minimal effects on the IM
241 alone. We observed that CBG (+polymyxin B) induced major permeability changes in the inner
242 membrane, indicated by a marked increase in optical density values due to ONPG hydrolysis as a result
243 of unmasking the cytoplasmic β -galactosidase, which can only occur with destabilization of IM, was
244 time dependent (Fig. 4c). CBG exhibited no action on the OM (Supplementary Fig. 6). Overall, the
245 mechanism of bacterial killing by CBG in *E. coli* is likely loss of IM integrity and requires antecedent
246 OM permeabilization.

247 Combination antibiotic therapy is becoming an increasingly attractive approach to combat
248 resistance³¹. So too is the strategy of using an OM perturbing molecule to facilitate the permeation of
249 compounds that are otherwise active only on Gram-positive bacteria³². We assessed the therapeutic
250 potential of the adjuvant polymyxin B in combination with CBG to inhibit the growth of priority Gram-
251 negative pathogens such as *A. baumannii*, *E. coli*, *Klebsiella pneumoniae*, and *Pseudomonas*
252 *aeruginosa* (Fig. 4d). We employed conventional checkerboard assays to determine the interaction and
253 potency of CBG and polymyxin B when used concurrently against various multi-drug resistant clinical
254 isolates. In all cases, synergy was evident, suggesting the potential for combination therapy of the
255 cannabinoids with polymyxin B against Gram-negative bacteria. Of note, the activity of CBG does not
256 seem to be affected by antibiotic-resistance mechanisms that are limiting the use of other antibiotics
257 and works effectively regardless of the susceptibility profile of the causative organism.

258 In summary, we have investigated the therapeutic potential of cannabinoids, and specifically
259 CBG, through a comprehensive study of *in vitro* potency on biofilms and persisters, as well as
260 mechanism of action studies and *in vivo* efficacy experiments. Most notably, we have uncovered the
261 hidden broad-spectrum antibacterial activity of cannabinoids and demonstrated the potential of CBG
262 against Gram-negative priority pathogens. Taken together, our findings lend credence to the idea that
263 cannabinoids may be produced by *Cannabis sativa* as a natural defense against plant pathogens.
264 Notwithstanding, cannabinoids are well-established as drug compounds that have favourable
265 pharmacological properties in humans. The work presented here suggests that the cannabinoid
266 chemotype represents an attractive lead for new antibiotic drugs.

267
268 **Acknowledgements** This work was supported by a salary award to E.D.B from the Canada Research
269 Chairs program and operating funds to E.D.B from a CIHR Foundation grant (FDN-143215); by
270 a Michael G. DeGroot Centre for Medicinal Cannabis Research post-doctoral fellowship to O.M.E.
271 Synthetic chemistry was supported by McMaster's Faculty of Health Sciences and the Michael G.
272 DeGroot Institute for Infectious Disease Research.

273 **Author contributions** M.A.F., O.M.E., R.T.G., and E.D.B. conceived and designed the research.
274 M.A.F. and O.M.E., performed all experiments and analyzed data with the exception of the mouse
275 infection model and the synthesis of CBG. C.R.M. and L.A.C. performed the mouse infection model.
276 X.Z. and N.G.J. optimized a scalable synthesis of CBG, supervised by J.M. M.A.F. and E.D.B. wrote
277 the paper, with large input from O.M.E. All authors approved the final version.

278 **Competing interests** E.D.B., J.M., M.A.F., O.M.E., and R.T.G. are inventors on a patent application
279 on the use of cannabinoids for prevention and/or treatment of infections.

280 METHODS

281 **Strains and reagents.** Supplemental Table 3 lists bacteria and plasmids used in this work. Bacteria
282 were grown in cation-adjusted Mueller Hinton broth (CAMHB) at 37°C, unless otherwise stated.
283 Cannabinoid standards and antibiotics were obtained from Sigma, Oakville, ON, Canada.

284 **Antimicrobial susceptibility testing.** Minimum inhibitory concentration (MIC) determination and
285 checkerboard assays were conducted following the guidelines of CLSI for MIC testing by broth
286 microdilution³³. When accurate MIC values could not be determined, the highest concentration tested
287 was considered to be half the MIC value. Fractional inhibitory concentration indices (FICI) were
288 calculated as $FICI = A/MIC_A + B/MIC_B$, where A and B are the concentrations of two antibiotics
289 required in combination to inhibit bacterial growth and MIC_A and MIC_B are the MIC values for drugs
290 A and B alone³⁴. FICI data were interpreted as 'synergy' ($FICI \leq 0.5$), 'antagonism' ($FICI > 4.0$), and
291 'no interaction or indifference' ($FICI 1-4.0$). Persister killing activity of cannabinoids was evaluated
292 against stationary-phase cells of *S. aureus* as previously described³⁵.

293 ***B. subtilis* CRISPRi essential gene knockdown strain collection screen.** Overnight cultures of the
294 collection²² (at a 96-well density, $n = 289$) were performed using the Singer rotor HDA (Singer
295 Instruments, United Kingdom) in CAMHB. Subsequently, CAMHB with or without CBG were
296 inoculated using the singer rotor at 96-well density. These experiments were performed either in the
297 presence of 0.05% xylose (allowing low level of *dcas9* expression) or with no xylose induction
298 (basal *dcas9* expression). The plates were incubated at 37°C and OD₆₀₀ was read after 24 h.

299 ***S. aureus* Nebraska Transposon Mutant Library (NTML) screen.** Overnight cultures of the
300 NTML²³ (at a 384-well density) were performed using the Singer rotor HDA (Singer Instruments,
301 United Kingdom) in CAMHB containing erythromycin (5 µg/mL). Subsequently, CAMHB with or
302 without CBG were inoculated using the singer rotor at 384-well density. The plates were incubated at
303 37°C and OD₆₀₀ was read after 24 h. Cellular localization and functional (gene ontology, GO-term)
304 enrichment analyses were performed using Pathway Tools software and MetaCyc database³⁶.

305 **Selection of suppressor mutants of CBG activity in *S. aureus*.** Spontaneous suppressor mutants were
306 selected for in liquid culture. Briefly, isolated colonies were resuspended in PBS and diluted to a final
307 OD₆₀₀ of 0.05 into 200 µL of CAMHB containing CBG (at 4x and 8x MIC) set up in 96-well microtiter
308 plates, 36 wells/concentration. Plates were incubated at 37°C for 4 days. Alternatively, bacteria were
309 treated with a 2-fold series of CBG concentrations spanning the MIC. Bacteria growing at the
310 maximum sub-MIC concentration were repeatedly passaged in a similar series of CBG concentrations
311 by 1000-fold dilution every 24 hours. Five CBG dilution series were performed simultaneously and the
312 cells were passaged for 15 days.

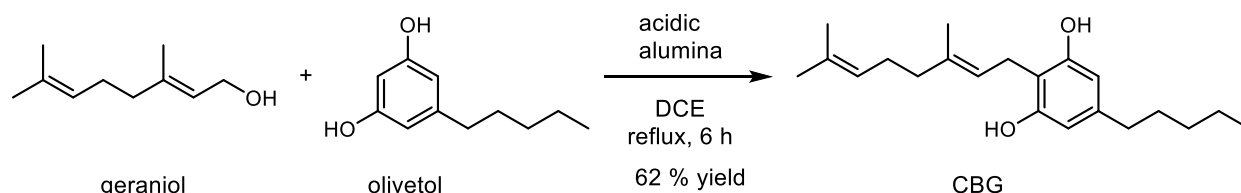
313 **General molecular techniques.** DNA manipulations were performed as previously described³⁷. CaCl₂
314 chemically-competent ML35 cells were transformed with pBR322 encoding a periplasmic β-lactamase.

315 **Biofilm formation assays.** Biofilm formation was performed in polystyrene 96-well plates in Tryptic
316 Soy Broth (TSB) with 1% glucose and detected by the crystal violet method as previously described³⁸.

317 **Membrane integrity assays.** DiSC₃(5) assay was performed in *S. aureus* as previously described³⁹. To
318 determine outer membrane and inner membrane activity of CBG against Gram-negative bacteria, we
319 performed β-lactamase and β-galactosidase assays, respectively. Overnight cultures of ML35 pBR322
320 in TSB with 50 µg/mL ampicillin were 100-fold diluted in fresh pre-warmed TSB and incubated at
321 37°C at 220 rpm. Logarithmic phase cells were collected, washed twice in PBS and then resuspended in
322 PBS at a final OD₆₀₀ of 0.01. Nitrocefin (30 µM) or ONPG (1.5 mM) - probes for β-lactamase and β-
323 galactosidase, respectively (final concentration) - were added to the bacterial suspension and
324 immediately aliquoted to dilution series of CBG and/or PMB at 100 µL final volume. Plates were
325 incubated at 37°C and monitored kinetically for color change at 492 and 405 nm (for nitrocefin and
326 ONPG hydrolysis, respectively). Adequate no drug, no probe and/or cell-free controls were included.

327 **Statistical analyses.** Statistical analyses were conducted with GraphPad Prism 5.0 and is indicated for
328 each assay in the figure caption. All results are shown as mean ±SEM unless otherwise stated. In the
329 case of MIC and checkerboard assays, the experiments were repeated at least three independent times
330 and the experiment showing the most conservative effects (if applicable) was shown and the mean
331 ±S.E.M. of the FICI was reported where applicable.

332 **Synthesis of Cannabigerol.** Chemical shifts in ¹H NMR and ¹³C NMR spectra are reported in parts
333 per million (ppm) relative to tetramethylsilane (TMS), with calibration of the residual chloroform peak
334 at δ_H 7.26, δ_C 77.16. Peak multiplicities are reported using the following abbreviations: s, singlet; t,
335 triplet; tq, triplet of quartets; m, multiplet. NMR spectra were recorded on a Bruker AVIII 700 NMR
336 spectrometer. ¹H NMR spectra were acquired at 700 MHz with a default digital resolution (Bruker
337 parameter: FIDRES) of 0.15 Hz/point, respectively. The ¹³C NMR (DEPTq) spectrum provided shows
338 CH and CH₃ carbon signals below the baseline and C and CH₂ carbons above the baseline. Olivetol
339 was purchased from Oakwood Chemical. Geraniol was purchased from AK Scientific. Aluminum
340 oxide (activated, acidic, Brockmann I) was purchased from Sigma-Aldrich. 1,2-dichloroethane (DCE),
341 ethyl acetate (EtOAc), and hexanes were purchased Fisher Scientific (certified ACS grade). Deuterated
342 chloroform was purchased from Cambridge Isotope Laboratories. All and solvents reagents were used
343 as received without further purification. Thin layer chromatography (TLC) was performed on Silicycle
344 TLC plates (0.2 mm) pre-coated with silica gel F-254 and visualized by UV quenching and staining
345 with *p*-anisaldehyde.
346



347

348

349

350

351

352

353

354

355

356

357

358

359

360

361

362

363

364

365

366

367

368

369

370

371

372

373

374

CBG was synthesized using a reported procedure⁴⁰. To a 25 mL round-bottomed flask containing a magnetic stir were added olivetol (108 mg, 0.6 mmol), chloroform (5 mL), geraniol (174 μ L, 1.0 mmol), *p*-toluene sulfonic acid monohydrate (19 mg, 0.1 mmol). The flask was covered with aluminum foil and the reaction was stirred at room temperature in the dark for 12 hours at which point TLC analysis indicated complete consumption of the olivetol substrate. To the reaction was added aqueous saturated NaHCO₃ (5 mL). The organic phase was removed and washed with water (5 mL). The aqueous layer was extracted with additional chloroform (5 mL) and the combined organic extracts were dried over MgSO₄ and concentrated *en vacuo*. The crude residue was purified via flash column chromatography on silica gel using gradient elution with hexanes and ethyl acetate. CBG was isolated as an off white powder in 28 % yield (54 mg, 0.17 mmol).

¹H NMR (700 MHz, CDCl₃) δ 6.25 (s, 2H), 5.28 (tq, J = 7.1, 1.3 Hz, 1H), 5.09 – 5.04 (m, 3H), 3.40 (d, J = 7.1 Hz, 2H), 2.49 – 2.43 (m, 2H), 2.14 – 2.04 (m, 4H), 1.82 (s, 3H), 1.68 (s, 3H), 1.60 (s, 3H), 1.58 – 1.54 (m, 2H), 1.36 – 1.28 (m, 4H), 0.89 (t, J = 7.0 Hz, 3H). ¹³C NMR (176 MHz, CDCl₃) δ 154.92, 142.89, 139.13, 132.19, 123.89, 121.84, 110.73, 108.52, 39.83, 35.65, 31.63, 30.93, 26.52, 25.81, 22.68, 22.40, 17.83, 16.32, 14.16.

Mouse infection models. Animal experiments were conducted according to guidelines set by the Canadian Council on Animal Care using protocols approved by the Animal Review Ethics Board at McMaster University under Animal Use Protocol #17-03-10. Before infection, mice were relocated at random from a housing cage to treatment or control cages. No animals were excluded from analyses, and blinding was considered unnecessary. Seven- to nine-week old female CD-1 mice (Envigo) were infected intraperitoneally with 7.5×10^7 CFU of log-phase MRSA strain USA 300 JE2 with 5% porcine mucin. Treatment of 100 mg/kg CBG or a vehicle solution (60% PEG300 and 5% DMSO) were administered intraperitoneally immediately post-infection. Mice were euthanized 7 hours post-infection and tissues collected into phosphate buffered saline (PBS) at necropsy. Organs were homogenized using a high-throughput tissue homogenizer, serially diluted in PBS, and plated onto solid LB. Plates were incubated overnight at 37°C and colonies were quantified to determine organ load.

374

375

References

375

376

377

378

379

380

381

382

383

384

385

386

387

388

389

390

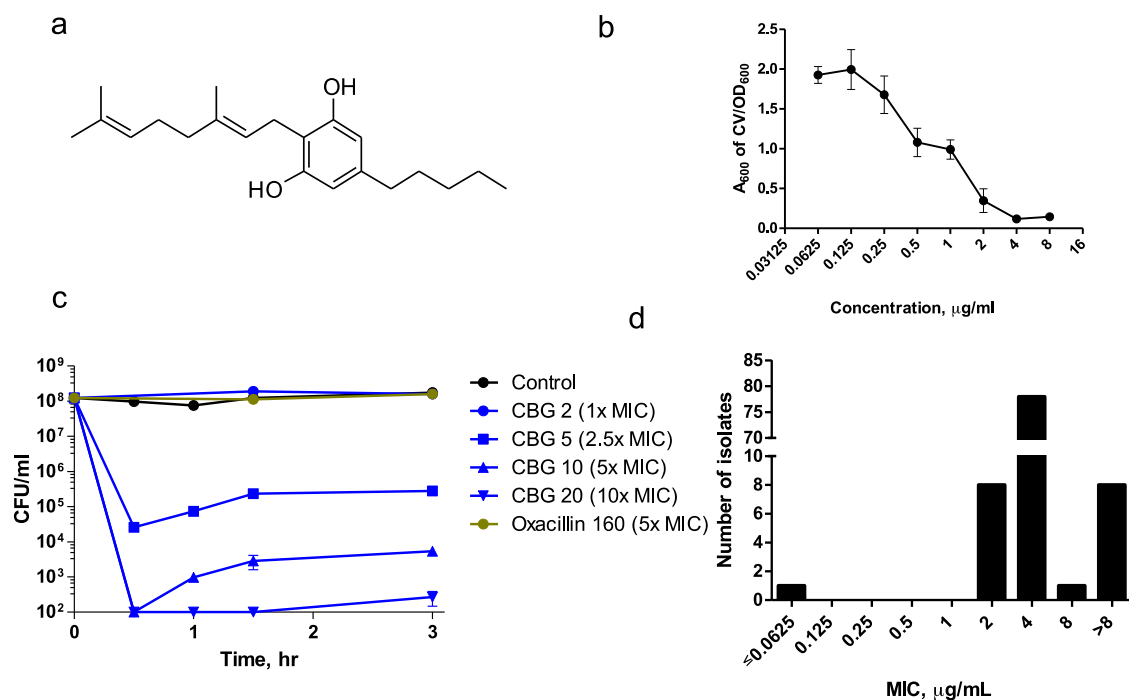
1. WHO *Global priority list of antibiotic-resistant bacteria to guide research, discovery, and development of new antibiotics*; World Health Organization: Geneva, 2017.
2. WHO *Prioritization of pathogens to guide discovery, research and development of new antibiotics for drug-resistant bacterial infections including tuberculosis*; World Health Organization: Geneva, 2017.
3. Boucher, H. W.; Talbot, G. H.; Bradley, J. S.; Edwards, J. E.; Gilbert, D.; Rice, L. B.; Scheld, M.; Spellberg, B.; Bartlett, J., Bad bugs, no drugs: no ESKAPE! An update from the Infectious Diseases Society of America. *Clin Infect Dis* **2009**, *48* (1), 1-12. DOI: 10.1086/595011.
4. Nannini, E.; Murray, B. E.; Arias, C. A., Resistance or decreased susceptibility to glycopeptides, daptomycin, and linezolid in methicillin-resistant *Staphylococcus aureus*. *Current opinion in pharmacology* **2010**, *10* (5), 516-21. DOI: 10.1016/j.coph.2010.06.006.
5. Goncalves, J.; Rosado, T.; Soares, S.; Simao, A. Y.; Caramelo, D.; Luis, A.; Fernandez, N.; Barroso, M.; Gallardo, E.; Duarte, A. P., Cannabis and Its Secondary Metabolites: Their Use as Therapeutic Drugs, Toxicological Aspects, and Analytical Determination. *Medicines (Basel)* **2019**, *6* (1). DOI: 10.3390/medicines6010031.

- 391 6. Appendino, G.; Gibbons, S.; Giana, A.; Pagani, A.; Grassi, G.; Stavri, M.; Smith, E.; Rahman,
392 M. M., Antibacterial cannabinoids from *Cannabis sativa*: a structure-activity study. *J Nat Prod* **2008**, *71*
393 (8), 1427-30. DOI: 10.1021/np8002673.
- 394 7. Van Klinger, B.; Ten Ham, M., Antibacterial activity of delta9-tetrahydrocannabinol and
395 cannabidiol. *Antonie Van Leeuwenhoek* **1976**, *42* (1-2), 9-12.
- 396 8. Turner, C. E.; Elsohly, M. A., Biological activity of cannabichromene, its homologs and
397 isomers. *J Clin Pharmacol* **1981**, *21* (S1), 283S-291S.
- 398 9. Blaskovich, M. A. T.; Kavanagh, A.; Ramu, S.; Levy, S.; Callahan, M.; Thurn, M., Cannabidiol
399 is a Remarkably Active Gram-Positive Antibiotic. *ASM Microbe Conference*, San Francisco, California,
400 2019.
- 401 10. Otto, M., Staphylococcal infections: mechanisms of biofilm maturation and detachment as
402 critical determinants of pathogenicity. *Annu Rev Med* **2013**, *64*, 175-88. DOI: 10.1146/annurev-med-
403 042711-140023.
- 404 11. Allison, K. R.; Brynildsen, M. P.; Collins, J. J., Metabolite-enabled eradication of bacterial
405 persisters by aminoglycosides. *Nature* **2011**, *473* (7346), 216-20. DOI: 10.1038/nature10069.
- 406 12. Davies, J.; Davies, D., Origins and evolution of antibiotic resistance. *Microbiol Mol Biol Rev*
407 **2010**, *74* (3), 417-33. DOI: 10.1128/MMBR.00016-10.
- 408 13. Lewis, K., Persister cells, dormancy and infectious disease. *Nat Rev Microbiol* **2007**, *5* (1), 48-
409 56.
- 410 14. Conlon, B. P., *Staphylococcus aureus* chronic and relapsing infections: Evidence of a role for
411 persister cells: An investigation of persister cells, their formation and their role in *S. aureus* disease.
412 *Bioessays* **2014**, *36* (10), 991-6. DOI: 10.1002/bies.201400080.
- 413 15. Lew, D. P.; Waldvogel, F. A., Osteomyelitis. *Lancet* **2004**, *364* (9431), 369-79. DOI:
414 10.1016/S0140-6736(04)16727-5.
- 415 16. Baddour, L. M.; Wilson, W. R.; Bayer, A. S.; Fowler, V. G., Jr.; Tleyjeh, I. M.; Rybak, M. J.;
416 Barsic, B.; Lockhart, P. B.; Gewitz, M. H.; Levison, M. E.; Bolger, A. F.; Steckelberg, J. M.; Baltimore,
417 R. S.; Fink, A. M.; O'Gara, P.; Taubert, K. A., Infective Endocarditis in Adults: Diagnosis, Antimicrobial
418 Therapy, and Management of Complications: A Scientific Statement for Healthcare Professionals
419 From the American Heart Association. *Circulation* **2015**, *132* (15), 1435-86. DOI:
420 10.1161/CIR.0000000000000296.
- 421 17. Keren, I.; Kaldalu, N.; Spoering, A.; Wang, Y.; Lewis, K., Persister cells and tolerance to
422 antimicrobials. *FEMS Microbiol Lett* **2004**, *230* (1), 13-8. DOI: S0378109703008565.
- 423 18. Conlon, B. P.; Rowe, S. E.; Gandt, A. B.; Nuxoll, A. S.; Donegan, N. P.; Zalis, E. A.; Clair, G.;
424 Adkins, J. N.; Cheung, A. L.; Lewis, K., Persister formation in *Staphylococcus aureus* is associated
425 with ATP depletion. *Nat Microbiol* **2016**, *1*, 16051. DOI: 10.1038/nmicrobiol.2016.51.
- 426 19. Andre, C. M.; Hausman, J. F.; Guerriero, G., *Cannabis sativa*: The Plant of the Thousand and
427 One Molecules. *Front Plant Sci* **2016**, *7*, 19. DOI: 10.3389/fpls.2016.00019.
- 428 20. Zheng, X. S.; Chan, T. F.; Zhou, H. H., Genetic and genomic approaches to identify and study
429 the targets of bioactive small molecules. *Chem Biol* **2004**, *11* (5), 609-18. DOI:
430 10.1016/j.chembiol.2003.08.011.
- 431 21. Barker, C. A.; Farha, M. A.; Brown, E. D., Chemical genomic approaches to study model
432 microbes. *Chem Biol* **2010**, *17* (6), 624-32. DOI: 10.1016/j.chembiol.2010.05.010.
- 433 22. Peters, J. M.; Colavin, A.; Shi, H.; Czarny, T. L.; Larson, M. H.; Wong, S.; Hawkins, J. S.; Lu,
434 C. H. S.; Koo, B. M.; Marta, E.; Shiver, A. L.; Whitehead, E. H.; Weissman, J. S.; Brown, E. D.; Qi, L.
435 S.; Huang, K. C.; Gross, C. A., A Comprehensive, CRISPR-based Functional Analysis of Essential
436 Genes in Bacteria. *Cell* **2016**, *165* (6), 1493-1506. DOI: 10.1016/j.cell.2016.05.003.
- 437 23. Fey, P. D.; Endres, J. L.; Yajjala, V. K.; Widhelm, T. J.; Boissy, R. J.; Bose, J. L.; Bayles, K.
438 W., A genetic resource for rapid and comprehensive phenotype screening of nonessential
439 *Staphylococcus aureus* genes. *MBio* **2013**, *4* (1), e00537-12. DOI: 10.1128/mBio.00537-12.
- 440 24. Hurdle, J. G.; O'Neill, A. J.; Chopra, I.; Lee, R. E., Targeting bacterial membrane function: an
441 underexploited mechanism for treating persistent infections. *Nat Rev Microbiol* **2011**, *9* (1), 62-75.
442 DOI: 10.1038/nrmicro2474.

- 443 25. Farha, M. A.; French, S.; Stokes, J. M.; Brown, E. D., Bicarbonate Alters Bacterial
444 Susceptibility to Antibiotics by Targeting the Proton Motive Force. *ACS Infect Dis* **2018**, *4* (3), 382-390.
445 DOI: 10.1021/acscinfecdis.7b00194.
- 446 26. Deiana, S.; Watanabe, A.; Yamasaki, Y.; Amada, N.; Arthur, M.; Fleming, S.; Woodcock, H.;
447 Dorward, P.; Pigliacampo, B.; Close, S.; Platt, B.; Riedel, G., Plasma and brain pharmacokinetic
448 profile of cannabidiol (CBD), cannabidivarin (CBDV), Delta(9)-tetrahydrocannabivarin (THCV) and
449 cannabigerol (CBG) in rats and mice following oral and intraperitoneal administration and CBD action
450 on obsessive-compulsive behaviour. *Psychopharmacology (Berl)* **2012**, *219* (3), 859-73. DOI:
451 10.1007/s00213-011-2415-0.
- 452 27. Delcour, A. H., Outer membrane permeability and antibiotic resistance. *Biochim Biophys Acta*
453 **2009**, *1794* (5), 808-16. DOI: 10.1016/j.bbapap.2008.11.005.
- 454 28. Krishnamoorthy, G.; Wolloscheck, D.; Weeks, J. W.; Croft, C.; Rybenkov, V. V.; Zgurskaya, H.
455 I., Breaking the Permeability Barrier of Escherichia coli by Controlled Hyperporination of the Outer
456 Membrane. *Antimicrob Agents Chemother* **2016**, *60* (12), 7372-7381. DOI: 10.1128/AAC.01882-16.
- 457 29. Powers, M. J.; Trent, M. S., Expanding the paradigm for the outer membrane: Acinetobacter
458 baumannii in the absence of endotoxin. *Mol Microbiol* **2018**, *107* (1), 47-56. DOI: 10.1111/mmi.13872.
- 459 30. Lehrer, R. I.; Barton, A.; Ganz, T., Concurrent assessment of inner and outer membrane
460 permeabilization and bacteriolysis in E. coli by multiple-wavelength spectrophotometry. *J Immunol*
461 *Methods* **1988**, *108* (1-2), 153-8.
- 462 31. Worthington, R. J.; Melander, C., Combination approaches to combat multidrug-resistant
463 bacteria. *Trends Biotechnol* **2013**, *31* (3), 177-84. DOI: 10.1016/j.tibtech.2012.12.006.
- 464 32. Stokes, J. M.; MacNair, C. R.; Ilyas, B.; French, S.; Cote, J. P.; Bouwman, C.; Farha, M. A.;
465 Sieron, A. O.; Whitfield, C.; Coombes, B. K.; Brown, E. D., Pentamidine sensitizes Gram-negative
466 pathogens to antibiotics and overcomes acquired colistin resistance. *Nat Microbiol* **2017**, *2*, 17028.
467 DOI: 10.1038/nmicrobiol.2017.28.
- 468 33. CLSI, *Methods for Dilution Antimicrobial Susceptibility Tests for Bacteria That Grow*
469 *Aerobically; Approved Standard—Ninth Edition. CLSI document M07-A9.* Clinical and Laboratory
470 Standards Institute: Wayne, PA, 2012.
- 471 34. Vaara, M.; Porro, M., Group of peptides that act synergistically with hydrophobic antibiotics
472 against gram-negative enteric bacteria. *Antimicrob. Agents Chemother.* **1996**, *40* (8), 1801-1805.
- 473 35. Kim, W.; Zhu, W.; Hendricks, G. L.; Van Tyne, D.; Steele, A. D.; Keohane, C. E.; Fricke, N.;
474 Conery, A. L.; Shen, S.; Pan, W.; Lee, K.; Rajamuthiah, R.; Fuchs, B. B.; Vlahovska, P. M.; Wuest, W.
475 M.; Gilmore, M. S.; Gao, H.; Ausubel, F. M.; Mylonakis, E., A new class of synthetic retinoid antibiotics
476 effective against bacterial persisters. *Nature* **2018**, *556* (7699), 103-107. DOI: 10.1038/nature26157.
- 477 36. Caspi, R.; Billington, R.; Fulcher, C. A.; Keseler, I. M.; Kothari, A.; Krummenacker, M.;
478 Latendresse, M.; Midford, P. E.; Ong, Q.; Ong, W. K.; Paley, S.; Subhraveti, P.; Karp, P. D., The
479 MetaCyc database of metabolic pathways and enzymes. *Nucleic Acids Res* **2018**, *46* (D1), D633-
480 D639. DOI: 10.1093/nar/gkx935.
- 481 37. Sambrook, J.; Fritsch, E. F.; Maniatis, T., *Molecular cloning: a laboratory manual.* 2nd ed.;
482 Cold Spring Harbor Laboratory: Cold Spring Harbor, New York, 1990.
- 483 38. Merritt, J. H.; Kadouri, D. E.; O'Toole, G. A., Growing and analyzing static biofilms. *Curr Protoc*
484 *Microbiol* **2005**, *Chapter 1*, Unit 1B 1. DOI: 10.1002/9780471729259.mc01b01s00.
- 485 39. Farha, M. A.; Verschoor, C. P.; Bowdish, D.; Brown, E. D., Collapsing the proton motive force
486 to identify synergistic combinations against *Staphylococcus aureus*. *Chem Biol* **2013**, *20* (9), 1168-78.
487 DOI: 10.1016/j.chembiol.2013.07.006.
- 488 40. Taura, F.; Morimoto, S.; Shoyama, Y., Purification and characterization of cannabidiolic-acid
489 synthase from Cannabis sativa L.. Biochemical analysis of a novel enzyme that catalyzes the
490 oxidocyclization of cannabigerolic acid to cannabidiolic acid. *J Biol Chem* **1996**, *271* (29), 17411-6.
491 DOI: 10.1074/jbc.271.29.17411.

492

493



494

495

496 **Fig. 1.** Cannabigerol (CBG) is a potent antibacterial, anti-biofilm and anti-persister cannabinoid. **a**, Chemical
 497 structure of CBG **b**, Concentration dependence for inhibition of MRSA biofilm formation by CBG. Shown is the
 498 average A_{600nm} measurements of crystal violet stained biofilms and normalized by the OD_{600} of planktonic cells
 499 with error bars representing one standard error of the mean, S.E.M. ($n=4$). **c**, Time-kill curve of *S. aureus*
 500 USA300 persisters by CBG compared to oxacillin shown as mean \pm S.E.M ($n=4$). CBG rapidly eradicated a
 501 population of $\sim 10^8$ CFU/ml MRSA persisters to below the detection threshold within 30 minutes of treatment .
 502 On the other hand, the β -lactam oxacillin at 160 μ g/mL (5x MIC) did not show any activity against the same
 503 population of persisters. **d**, MIC_{90} distribution of CBG against clinical isolates of MRSA ($n=96$). The MIC_{90} is 4
 504 μ g/mL.

505

506

507

508

509

510

511

512

513

514
515
516
517
518
519
520
521
522
523
524
525
526
527
528
529
530
531
532
533
534
535
536
537
538
539
540
541
542

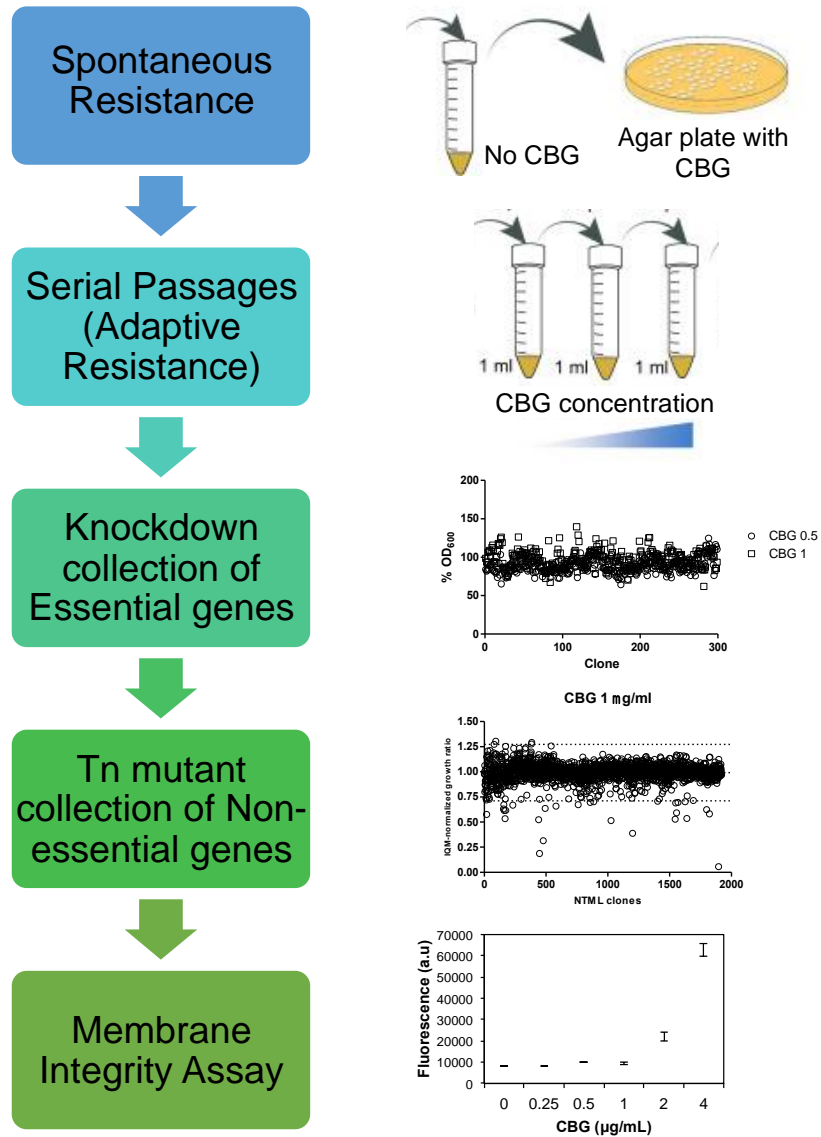


Fig. 2. CBG is active on the cytoplasmic membrane of MRSA. Overview of strategies for mechanism of action determination, culminating in the finding that CBG is active on the cytoplasmic membrane, as determined by dose-dependent increases in DiSC₃(5) fluorescence.

543
544
545
546
547
548
549
550
551
552
553
554
555
556
557
558
559
560
561
562
563
564
565
566
567
568
569
570
571

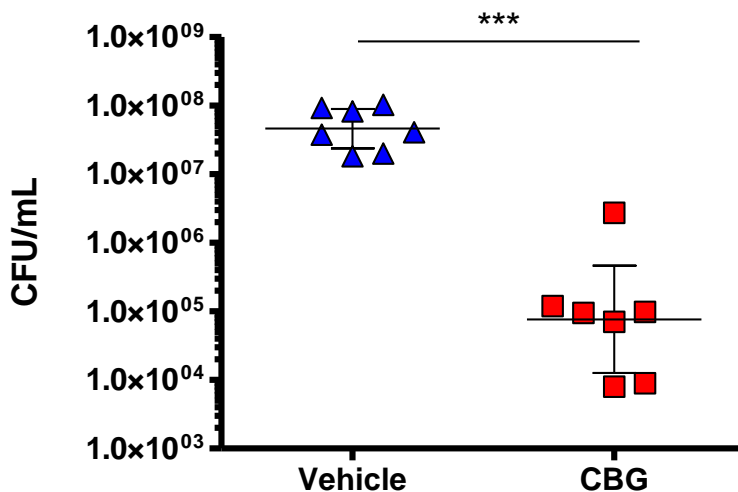
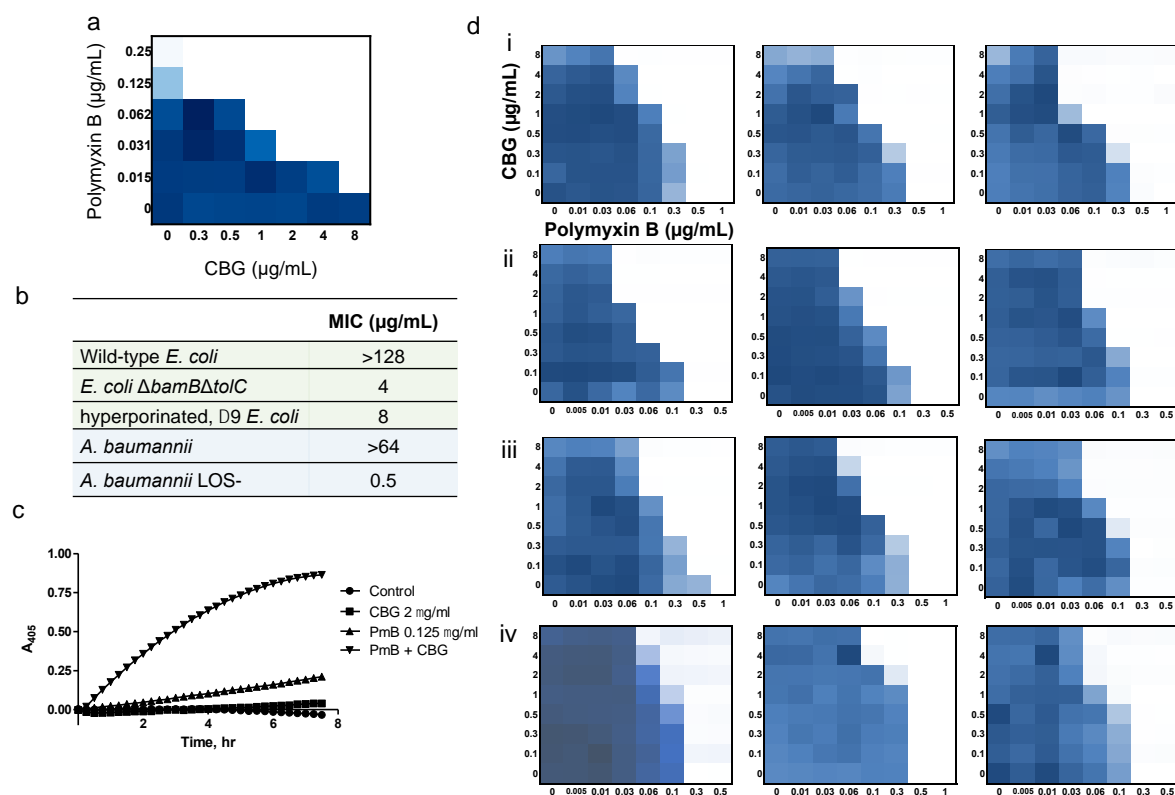


Fig. 3. CBG is efficacious in a systemic mouse model of *S. aureus* infection when administered single-dose treatment immediately post infection of CBG (n=7, red, 100 mg kg⁻¹, i.p.) or vehicle control (n=7, blue, i.p.). Colony-forming units (CFU) within spleen tissue were enumerated at 7 h post infection. Horizontal lines represent the geometric mean of the bacterial load for each treatment group. Administration of CBG resulted in a 2.8-log₁₀ reduction ($p < 0.001$, Mann–Whitney *U*-test) in CFU when compared to the vehicle control.



572

573

574 **Fig. 4.** CBG is active against Gram-negative bacteria whose outer membrane is permeabilized, where it acts on
 575 the inner membrane. **a**, Checkerboard analysis of CBG in combination with polymyxin B against *E. coli*. The
 576 extent of inhibition is shown as a heat plot, such that the darkest blue color represents full bacterial growth. **b**,
 577 CBG becomes active against Gram-negative bacteria in various genetic backgrounds where the outer membrane
 578 is compromised. **c**, CBG acts on the IM of *E. coli* but only in the presence of sub-lethal concentration of
 579 polymyxin B (PmB), unmasking cytoplasmic β -galactosidase leading to hydrolysis of ONPG as detected via
 580 absorbance reads at 405 nm over time. **d**, CBG in combination with polymyxin B against multi-drug resistant
 581 clinical isolates of i, *A. baumannii*, ii, *E. coli*, iii, *K. pneumoniae*, iv, *P. aeruginosa*. The extent of inhibition is
 582 shown as a heat plot, such that the darkest blue color represents full bacterial growth.

583

584

585

586

587

588

589